Renal Failure

ISSN: 0886-022X (Print) 1525-6049 (Online) Journal homepage: https://www.tandfonline.com/loi/irnf20

Inhalation of mercury vapor can cause the toxic effects on rat kidney

Nilgün Akgül, Berrin Zuhal Altunkaynak, Muhammed Eyüp Altunkaynak, Ömür Gülsüm Deniz, Deniz Ünal & Hayati Murat Akgül

To cite this article: Nilgün Akgül, Berrin Zuhal Altunkaynak, Muhammed Eyüp Altunkaynak, Ömür Gülsüm Deniz, Deniz Ünal & Hayati Murat Akgül (2016) Inhalation of mercury vapor can cause the toxic effects on rat kidney, Renal Failure, 38:3, 465-473, DOI: 10.3109/0886022X.2016.1138832

To link to this article: https://doi.org/10.3109/0886022X.2016.1138832

Published online: 18 Feb 2016.

RENAL FAILURE, 2016
VOL. 38, NO. 3, 465–473
http://dx.doi.org/10.3109/0886022X.2016.1138832

Taylor & Francis
Taylor & Francis Group

LABORATORY STUDY

Inhalation of mercury vapor can cause the toxic effects on rat kidney

Nilgün Akgül[a], Berrin Zuhal Altunkaynak[b], Muhammed Eyüp Altunkaynak[b], Ömür Gülsüm Deniz[b], Deniz Ünal[c] and Hayati Murat Akgül[d]

[a]Department of Restorative Dentistry, School of Dentistry, Atatürk University, Erzurum, Turkey; [b]Department of Histology and Embryology, School of Medicine, Ondokuz Mayis University, Samsun, Turkey; [c]Department of Histology and Embryology, School of Medicine, Atatürk University, Erzurum, Turkey; [d]Department of Oral Diagnosis and Radiology, School of Dentistry, Atatürk University, Erzurum, Turkey

ABSTRACT

Dental amalgam has been used in dentistry as a filling material. The filler comprises mercury (Hg). It is considered one of the most important and widespread environmental pollutants, which poses a serious potential threat for the humans and animals. However, mercury deposition affects the nervous, cardiovascular, pulmonary, gastrointestinal, and especially renal systems. In most animals' species and humans, the kidney is one of the main sites of deposition of mercury and target organ for its toxicity. In this study, the effects of mercury intake on kidney in rats were searched. For the this purpose; we used 24 adult female Wistar albino rats (200 g in weight) obtained from Experimental Research and Application Center of Atatürk University with ethical approval. Besides, they were placed into a specially designed glass cage. Along this experiment for 45 days, subjects were exposed to (1 mg/m^3/day) mercury vapor. However, no application was used for the control subjects. At the end of the experiment, kidney samples were obtained from all subjects and processed for routine light microscopic level and stereological aspect were assessed. Finally, according to our results, mercury affects the histological features of the kidney. That means, the severe effects of mercury has been shown using stereological approach, which is one of the ideal quantitative methods in the current literature. In this study, it was detected that chronic exposure to mercury vapor may lead to renal damage and diseases in an experimental rat model.

ARTICLE HISTORY
Received 27 August 2015
Accepted 21 December 2015
Published online
11 February 2016

KEYWORDS
Histopathology; kidney; mercury vapor; rat; stereology

Introduction

Mercury is a widespread environmental and industrial pollutant, which induces severe alterations in the body tissues of both humans and animals.[1] This element is released in the environment by human activity, such as mining, smelting, extensive industrial and agricultural usage, combustion of fossil fuels, and other industrial release. On population level, Hg released into the environment and dental amalgam is a major exposure source.[2,3] It enters the body in variety of chemical forms that are elemental and inorganic.[4,5] Mercury is a well-known toxic heavy metal, producing toxicity to the kidney, brain, liver, the reproductive systems, and other organs.[6] The kidneys are the primary target organ where inorganic mercury is taken up, accumulated, and expresses toxicity.[7] In the kidneys, the toxicity of inorganic mercury is related to its accumulation in the epithelial cells from the proximal tubules, and with its binding to intracellular sulfhydryl, carboxyl, and phosphoryl groups.[8] The results of these interactions are enzymatic inactivation, inhibition of protein synthesis,[9] inhibition of the cellular multiplication, decrease in the uridine and thymidine uptake, DNA fragmentation, and cellular death.[10] Inorganic mercury alters the content of intracellular thiols and in this manner it induces oxidative stress, lipid peroxidation, mitochondrial dysfunction, and changes in the metabolism of heme.[11] Many research groups have associated morphologic changes within the kidney when cells are intoxicated with heavy metals.[12,13] The principal target of mercury toxicity is the *pars recta* (segment S3) from the proximal tubule, particularly the portion at the junction of the cortex and the outer medulla.[14] There have been numerous studies dedicated to the study of mercury toxicity.

In this study, it was aimed to do stereological estimations on kidney volume, volume of cortex, volume of medulla, volume of distal tubule, volume of proximal tubule, volume of glomeruli, numerical density of glomeruli and total number of glomeruli. For this aim,

CONTACT Dr Berrin Zuhal Altunkaynak, PhD berrinzuhal@gmail.com Department of Histology and Embryology, Medical Faculty, Ondokuz Mayis University, 55139 Samsun, Turkey

volumetric values and numerical data were estimated via Cavalieri and physical dissector method. Also, in this study, histological examination was made at light and electron microscopic levels.

Materials and methods

In this study, 24 Wistar albino adult rats (12 male, 12 female, 200 g in weight) were used. The subjects were exposed to (1 mg/m^3/day) mercury vapor in a specially-designed lantern during 45 days. Pressure of mercury in lantern was designed similar to the Faculty of Dentistry clinic (48.7 μg/m^3). No applications were made for the control subjects in the same lantern. At the end of the experiment, kidney samples were obtained from all subjects histologically assessed according to routine light and electron microscopical and also stereological procedures.

Microscopy

Kidney samples for light microscopic examination were fixed in 10% formaldehyde, dehydrated in a graded alcohol series, and cleared in xylene. After dehydration, specimens were embedded in fresh paraffin (Agar, Cambridge, UK). Sections were cut using a microtome (Leica, Nussloch, Germany). Each paraffin block was serially cut to 5-μm thickness. Approximately 100 sections were obtained from each tissue block. The sections were stained with hematoxylin-eosin (H-E) for light microscopic examination and stereological analysis.

For electron microscopic examination, kidneys were fixed in buffered 3% glutaraldehyde in 0.1 M phosphate, post-fixed in 1% osmium tetroxide, dehydrated in a graded acetone series, and transferred to propylene oxide. After dehydration, specimens were embedded in Araldite CY 212. Sectioning, staining, and examination of the samples were done as previously.

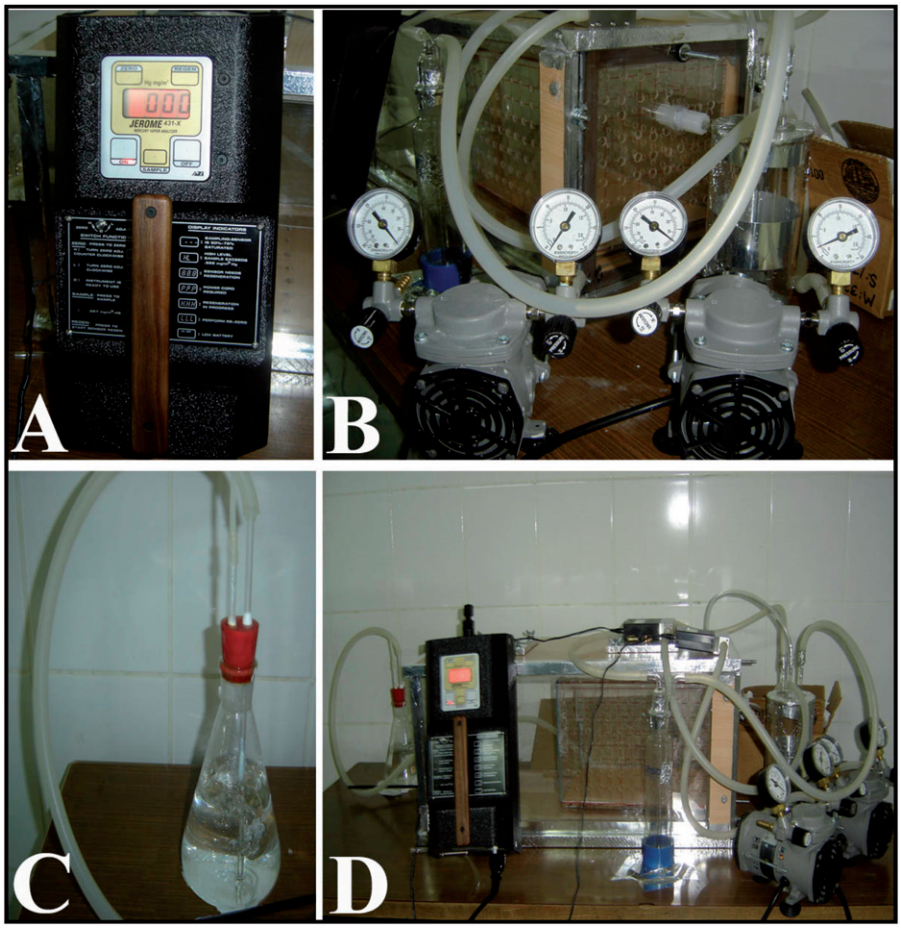

Figure 1. Specially designed lantern for mercury vapor application. A; special machine for measurement of vapor pressure, B; special lantern with manometers, C; nitric acid pot for elimination of waste of the mercury, D; completely view of the lantern.

Volume of cortex, volume of medulla, and volume of glomeruli and tubules

We used 15–20 sections obtained for application of the Cavalieri method to estimate the volume of the cortex, medulla, glomeruli, and the distal and proximal tubules, and their fraction of whole kidney volume.[15] For this purpose; two different point-counting test grids were used. The point density of the point-counting grids, which are designed to hit a minimum of 1000 points per region of interest (cortex, medulla, glomeruli, and tubules), for each animal was appropriate to obtain a significant coefficient of error (CE).[16,17] CE and coefficient of variation (CV) were estimated according to two different point-counting grids were composed of dense and loose points according to the area of interest.[18] Grids with a systematic array were randomly placed on the PC screen; the hitting point of the grid on all subjects of interest was counted.

The loose points were used to estimate the volume fraction of the cortex and medulla and the dense points were used for the volume fraction of glomeruli, Bowman's space, and tubules. Sampled areas were chosen in a systematic random manner by means of a motorized stage. The total number of points that were superimposed on each area of interest was counted. Subsequently, the volumes of the structures of interest in each section were estimated from the following equation:

$$\text{Volume } (V) = t\,x\,a\,(p) \times (p)$$

where V is the volume of interest (kidney, glomerulus, tubules) in one section plane, t is the section thickness, a/p is the interpoint area, and P is the number of points hitting the object of interest in that section. After this formula was applied to other sections, the total volume to be estimated was obtained from:

$$\text{Total volume} = V1 + V2 + \ldots + Vn$$

The volume fractions for each region were estimated by dividing the total point number that was superimposed on the related region by the sum of the points superimposed on the whole kidney:

$$\text{volume fraction}(\text{region}/\text{kidney}) = P(\text{region})/P(\text{kidney})$$

where P is the number of points hitting the region of interest or whole kidney in that section.

Numerical density and total number of glomeruli

In a study was described selection of the physical dissector pairs.[19] Based on the findings obtained from a pilot study, the first chosen section and its adjacent section, called a dissector pair, were separated by a distance of 30 μm (thickness of seven sections: 35-μm distance) as a rule of the physical dissector. According to this rule, the distance between the section pairs must be about 30–40% of the average projected height of the object of interest to be estimated in this way, approximately 15–20 section pairs were obtained and evaluated.

This number is in an acceptable range for stereological analysis.[20,21] Two consecutive sections were mounted on each slide. Photographs of adjacent sections were taken with a digital camera at a magnification of 400. An unbiased counting frame was placed on the reference and the look-up sections on the screen of the PC, to perform the counting according to the dissector method.[21] The bottom and the left-hand edges of the counting frame were considered to be the forbidden (exclusion) lines together with the extension lines. Other boundaries of the frame that are the top-right edges were considered to be inclusion lines, and any particle that hit these lines or was located inside the frame was counted as a dissector particle. The size of the unbiased counting frame was adjusted to count ~600 glomeruli from each sample.

The dimension of the counting frame on the PC screen was $20 \times 20\,\text{cm}^2$, and the real dimension of this counting frame ($1\,\text{cm}^2$) was estimated by the following formula:

$$\text{Real dimension} = \text{screen size of frame}/\text{total magnification of microscope.}$$

Glomeruli seen in the reference section but not in the look-up section were counted.[20] The mean numerical density of glomeruli [Nv (glomeruli)] per cm^3 was estimated using the following formula:

$$Nv\ (\text{glomeruli}) = Q^{-}(\text{glomeruli})/tA$$

where Q is the total number of glomeruli counted in the reference section, t is the mean section thickness (5 μm), and A is the area of the unbiased counting frame. Thus, the total number of glomeruli [TN (glomeruli)] in a whole rat kidney was estimated by the following equation:

$$TN\ (\text{glomeruli}) = Nv\ (\text{glomeruli}) \times \text{kidney volume}$$

where Nv (glomeruli) is the numerical density of glomeruli per cm^3, TN (glomeruli) is the total number of glomeruli in the whole kidney calculated by using Nv (glomeruli) and the kidney volume results estimated by the Cavalieri method. Finally, histopathological examinations were carried out on images of the same sections.

Statistical analysis

Differences in volumetric data, numerical density, total number or glomerular height between the two groups

were tested using the independent samples *t*-test (two tailed, with a significance limit of $p = 0.05$ in this test). All statistical calculations were performed using SPSS 13.0 software (Chicago, IL) for Windows.

Results

Stereological results

Stereological findings of the study are summarized in Figure 1. Stereological findings showed that the mean numerical density of glomeruli for the control group was significantly higher than the Hg group ($p < 0.01$). Total number of glomeruli for the control group were significantly higher than the Hg group ($p < 0.01$). Besides, the mean volume of distal tubule for the Hg group were significantly higher than the control group ($p < 0.01$). The mean volume of proximal tubule of the control group were significantly higher than the Hg group ($p < 0.01$). In addition, mean volume of glomeruli of control and Hg groups showed significant difference at $p < 0.05$. All stereological results are summarized in Tables 1 and 2, and Figures 2 and 3.

Table 1. Mean volume and numerical data of glomeruli in both groups.

	Groups	
Estimations	Control	Hg
Mean numerical density of glomeruli (Glomeruli/cm^3)	279,710 ± 8391	265,987 ± 4779
Total number of glomeruli	332,333 ± 9969	310,580 ± 8117
Mean volume of glomeruli (μm^3)	698,400 ± 20,952	564,700 ± 16,941

Table 2. Mean volume of all kidney, cortex, medulla, and tubules in both groups.

	Groups	
Estimations	Control	Hg
Mean volume of kidney (cm^3)	2.15 ± 0.27	1.84 ± 0.11
Mean volume of cortex (cm^3)	1.74 ± 0.14	1.37 ± 0.095
Mean volume of medulla (cm^3)	0.363 ± 0.042	0.47 ± 0.054
Mean volume of distal tubule (mm^3)	0.0012 ± 0.00087	0.0042 ± 0.00072
Mean volume of proximal tubule (mm^3)	0.00413 ± 0.00078	0.00255 ± 0.000082

Histological results

Light microscopy

Histopathological findings of kidneys were consistent with each other in the Hg group, such as vacuolar changes and pyknotic nuclei of glomerular and tubular cells, and also tubular necrosis were observed in mercury vapor inhaled rats (Figure 4). On the other hand, glomerular sclerosis and glomerular degeneration was seen in the Hg group. It is observed that Bowman's space was dilated according to the control group (Figure 4). Besides, at light microscopy of renal tissue samples obtained from the Hg group, the cells which are stained darkly cytoplasm were observed. Moreover, collecting tubules that were indistinguishable from the cytoplasm borders were observed, tubules with dead cell and structures were the possible residue of dead cells (Figure 5). Also, no pathological change was observed in the control group (Figure 6).

Electron microscopy

Electron microscopic (EM) examination of the Hg group kidney samples demonstrated pathological changes in distal tubule cells, podocytes and mesangial cells. Also, tubule cells included progressively degenerated mitochondria. Nucleus of these tubular cells was electron lucent and appears to have dispersed chromatin. But, distal tubule cells of the control group had normal appearance (Figure 7).

Damaged appearance of glomerular cells and basement membrane in the Hg group was observed, so

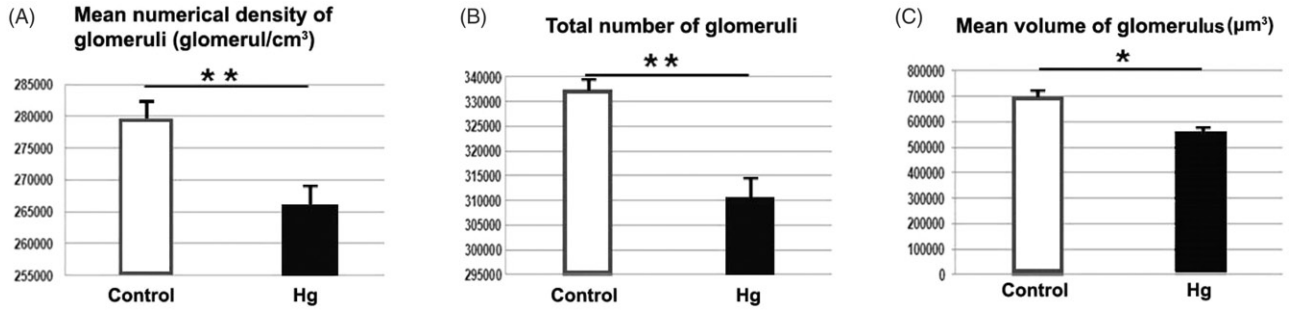

Figure 2. A: Mean numerical density of glomeruli belongs to control and Hg groups are shown. Mean numerical density of glomeruli for the control group were significantly higher than the Hg group (**$p < 0.001$). B: Total number of glomeruli belongs to control and Hg groups are shown. Total number of glomeruli for the control group were significantly higher than the Hg group (**$p < 0.001$). C: Mean volume of glomeruli belongs to control and Hg groups are shown. *shows that significant difference between groups ($p < 0.005$).

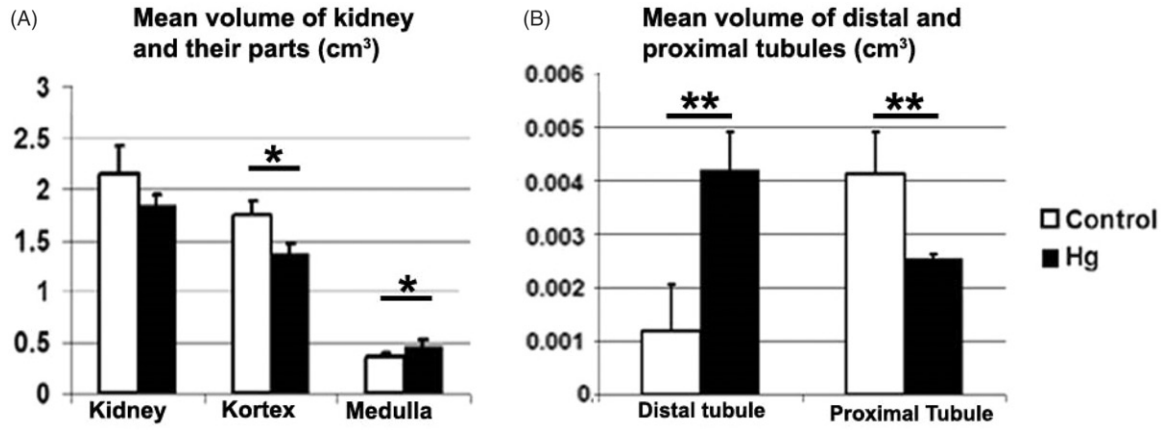

Figure 3. A: The mean volume of kidney and kidney's parts belongs to control and Hg groups are shown. B: The mean volume of distal and proximal tubules belongs to control and Hg groups are shown. The mean volume of distal tubule for the Hg group were significantly higher than the control group (**$p < 0.001$). The mean volume of proximal tubule for control were significantly higher than the Hg group (**$p < 0.001$).

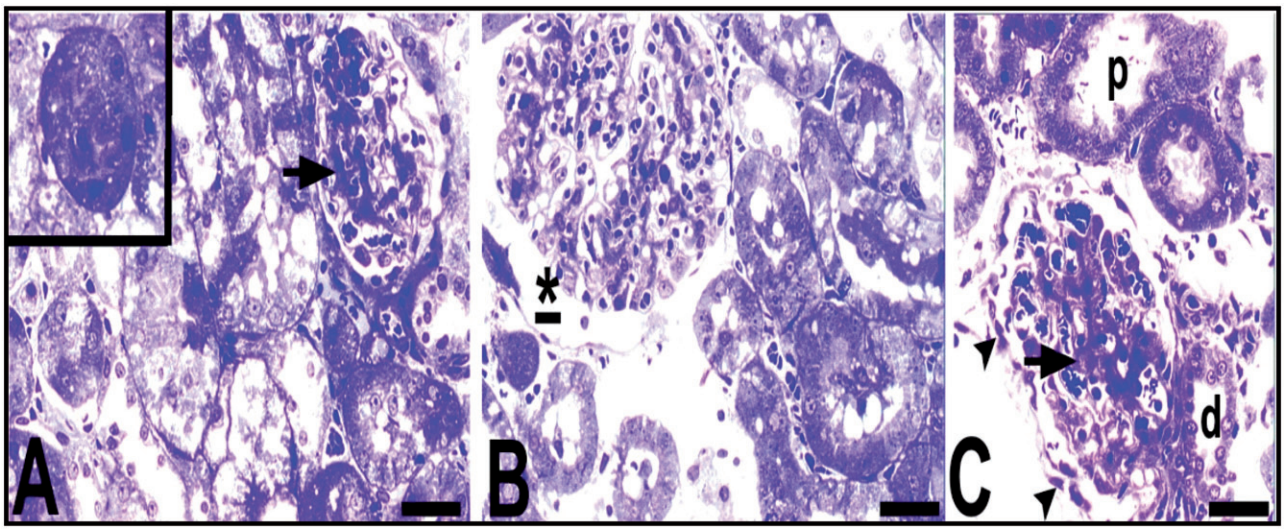

Figure 4. Light microscopy of renal tissue samples which are obtained from the Hg group. Arrow (A), glomerular sclerosis; *Bowman's space which enlarged according to the control group (B); arrow and arrow head (C), glomerular degeneration and degenerated podocyte, respectively; p, proximal tubule; d, distal tubule (C). Bars show 50 μm. Inset shows necrotic tubule.

podocytes have vacuolar degenerations, irregular cell and nuclear boundaries, and hyperchromatic nuclei. Besides, pedicels of the cells were different from those of the control group and they have irregular boundaries too. In the Hg group, glomerular basement membrane was thickened and it had irregular cell lines. Also, in the Hg group, mesangial cells had hyper chromatic nucleus (Figure 8). All of the cells had cytoplasmic disorganization (Figures 7 and 8).

Discussion

Multiple pathways of mercury through air, food, water, pharmaceuticals, cosmetics, etc., account for its easy accessibility to man, factors like bio-magnification of mercury along the food chain complicate the problem.[22] Mercuric ion, one of strongest thiol-binding agents,[22] is known to increase the intracellular levels of reactive oxygen species and induce oxidative stress[23] resulting in tissue damage.[24] Toxicity of this metal is associated with superoxide radical generation and glutathione depletion.[25,26] Findings reported earlier indicate that alterations in antioxidant enzyme activities in mercury intoxication is due to the generation of reactive oxygen species (O_2 or H_2O_2) leading to enhancement in lipid peroxidation levels and depletion in glutathione levels. Cantoni et al.[27] and Chung et al.[28] have reported significant reduction in glutathione levels in liver and

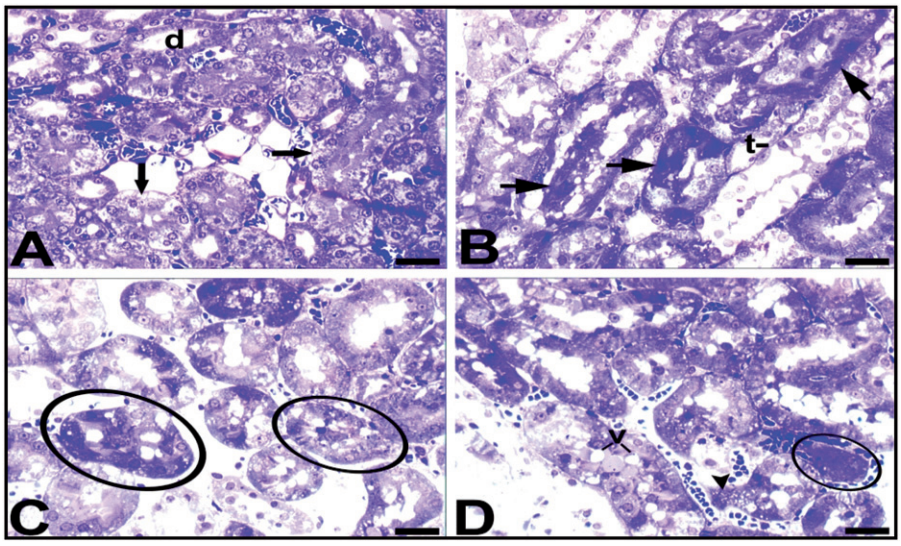

Figure 5. Light microscopy of renal tissue samples which are obtained from the Hg group. d, distal tubule; arrow (A), tubule cells with hydropic degeneration; arrow (B), cells with the damaged-looking which are stained darkly cytoplasm and pycnotic nuclei; t, collecting tubules with indistinguishable cytoplasmic borders; v, (D) vacuoles; arrow head, (D) a degenerated tubule cell with micro vacuoles and disappeared nucleus. Circled areas show tubules with dead cell in C and structures are possible residue of dead cells in D. Bars show 50 μm.

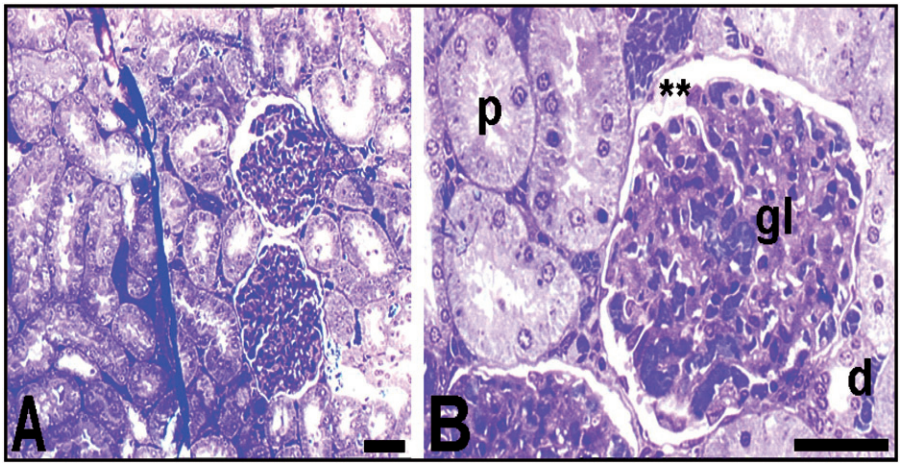

Figure 6. Light microscopy of renal tissue samples which obtained from control group. The general appearance of the kidney of the control group (A); p, proximal tubule; d, distal tubule; gl, glomerulus; **Bowman's space (B). Bars show 50 μm.

kidney tissues, while Gastraunthaler et al.[29] have also reported depletion in renal superoxide dismutase, glutathione peroxidase and catalase activities and glutathione levels.

Experiments performed on various experimental animals showed that mercury released from dental amalgam fillings markedly increased the concentration of mercury in various tissues, most prominently in the kidneys, brain, pituitary, and pulpa.[30–33] There are numerous studies establishing mercury toxicity as occupational health hazard for gold miners, chloral kali workers, and dental personnel.

The kidney appears to be the critical organ of toxicity for the ingestion of mercuric salts. Several widespread alterations were observed in kidney from Hg-intoxicated mice. In the literature, there are many studies about kidney structure. Some of these articles are performed with histopathological or biochemical methods. However, the number of quantitative and/or embryological studies that were made with unbiased

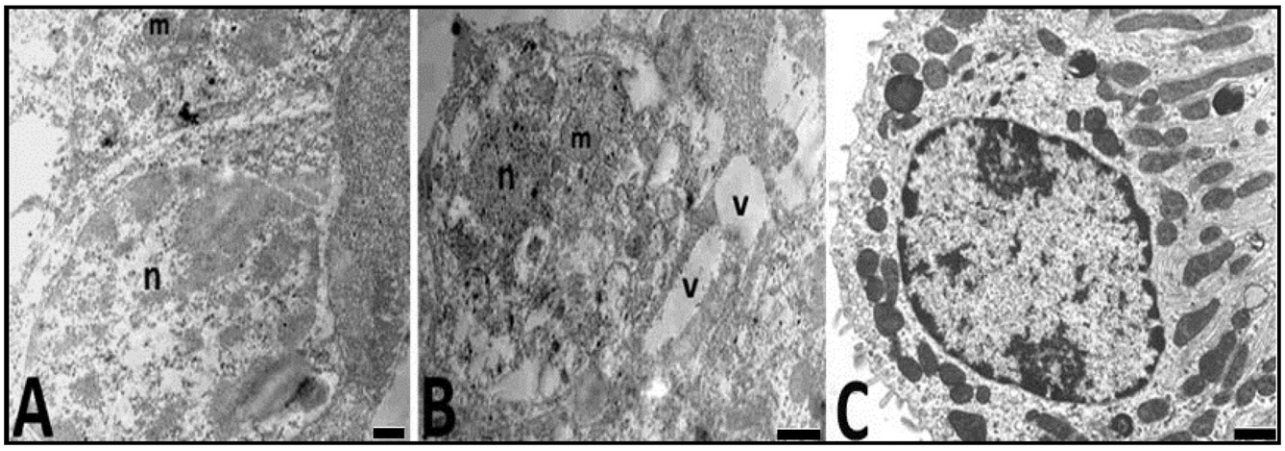

Figure 7. Electron micrographs of the distal tubule cells of animals from the control (C) and Hg (A, B) groups are seen. n, nucleus and m; mitochondria in the control group (A). nucleus (n), mitochondria (m), and vacuole (v) distal tubule cells have damaged appearance in the experimental group (A, B). Bars show 0.5 μm.

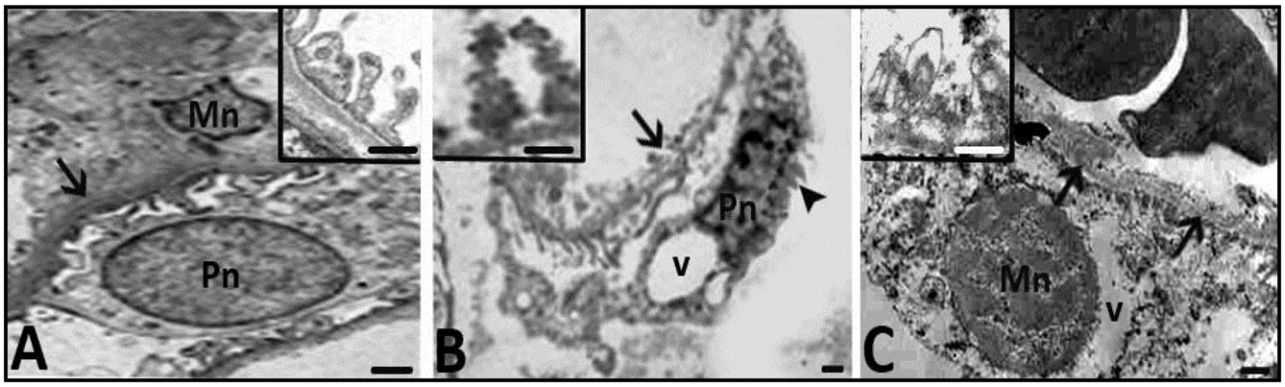

Figure 8. Electron micrographs belonging to the control (A) and Hg (B,C) groups are seen. Mn; nucleus of mesengial cell, Pn; nucleus of podocyte. EM pictures in B and C show that damaged appearance of mesangial cells and podocytes with irregular membrane and nuclear contours (arrow head), hyperchromatic nuclei and also thickened and degenerated basement membrane (arrows and inset in C). Inset in B shows pedicels having irregular boundaries in Hg group. Bars show 0.5 μm.

stereological methods is few.[34] Moreover, there are few descriptions focused on kidney alterations in mercury-intoxicated rats. For example; Agarwal et al.[35] demonstrated that Hg is a nephrotoxic element. Moreover, Eto et al.[36] detected Hg in renal tubules causes glomerular fibrosis. It is well established that *pars recta* (straight segment) of the proximal tubule (particularly the portion at the junction of the cortex and outer medulla) is the segment of the nephron that is most vulnerable to the toxic effects of both inorganic and organic forms of mercury.[37,38] But, there are a few study demonstrating the effects of mercury vapor on kidney at microscopic level. Also, there was no stereological study basing to unbiased gold standard data. So, in the current study, we determined toxicity of Hg vapor on rat kidney with stereological and histological approaches. Our stereological analysis included mean numerical density of glomeruli, total number of glomeruli, and mean volume of glomeruli, kidney, cortex, medulla, distal tubule, and proximal tubule. Our histological evaluations were made at light and electron microscopic levels.

According to our results; the mean number of glomeruli of subjects exposed to mercury vapor was significantly decreased than in controls ($p < 0.05$). This group has also reduced average volumes of the proximal and distal tubules according to the control group ($p < 0.05$).

In light microscopical analysis, vacuolar changes and pyknotic nuclei of glomerular and tubular cells, and also tubular necrosis were observed in mercury vapor inhaled rats. On the other hand, glomerular sclerosis and glomerular degenerations was seen in the experimental group. It is observed that Bowman's space was dilated according to the control group. Besides, at light

microscopy of renal tissue samples that are obtained from the experimental group, the cells which are stained darkly cytoplasm are observed. Moreover, it was seen collecting tubules that are indistinguishable from the cytoplasm borders, tubules with dead cell, and structures are possible residue of dead cells. Some of these data were published in the literature after HgCl administration.[39,40]

When kidney samples were evaluated under light microscopy, it was detected that histopathological findings were consistent with stereological results of the study. We thought that the number of glomeruli was decreased due to glomerular sclerosis and may be segmental or total necrosis. Also, decreased volumes of both proximal and distal tubules are caused from tubular necrosis. Mean volume of glomerulus was not changed because volumes of Bowman spaces were enlarged in surviving glomeruli.

The ultrastructural features of the kidney cells have been described in the literature.[41] They have indicated that Hg caused death of some cells by necrosis, cytoplasmic disorganization, and large vacuoles in cell culture. In the present EM examination in the Hg group, it was found that vacuole and nucleus and mitochondria of tubule cells have a damaged appearance. Not only the tubule cells have damaged appearance, but also this situation was seen in the podocytes, mesangial cells, and glomerular basement membrane as *in vivo*.

Finally, present work demonstrated the nephrotoxicity of Hg vapor with stereological and detailed light and electron microscopical analyses.

Disclosure statement

The authors report no conflicts of interest.

References

1. Mahboob M, Shireen KF, Atkinson A, Khan AT. Lipid peroxidation and antioxidant enzyme activity indifferent organs of mice exposed to low level of mercury. *J Environ Sci Health B*. 2001;36(5):687–697.
2. Papp A, Nagymajtényi L, Vezér T. Subchronic mercury treatment of rats in different phases of ontogenesis: Functional effects on the central and peripheral nervous system. *Food Chem Toxicol*. 2005;43(1):77–85.
3. Trepka MJ, Heinrich J, Krause C. Factors affecting internal mercury burdens among eastern German children. *Arch Environ Health*. 1997;52(2):134–138.
4. Clausen J. Mercury and multiple sclerosis. *Acta Neurol Scand*. 1993;87(6):461–464.
5. Gasso S, Sunol C, Sanfeliu C, Rodriguez-Farre E, Cristofol RM. Pharmacological characterization of the effects of methyl mercury & mercuric chloride on spon-taneous nonadrenaline release from rat hippocampal slices. *Life Sci*. 2000;67(10):1219–1231.
6. Liu J, Goyer R, Waalkes MP. Toxic effects of metals. In: Klaassen CD, ed. *Casarett and Doull's Toxicology. The Basic Science of Poisons*. 7th ed. New York: McGraw Hill; 2008:931–979.
7. Zalups RK. Molecular interactions with mercury in the kidney. *Pharmacol Rev*. 2000;52(1):113–143.
8. Goyer RA. Toxic effects of metals. In: Klaassen CD, ed. *Casarett and Doull's Toxicology. The Basic Science of Poisons*. 5th ed. New York: McGraw-Hill; 1996:709–712.
9. Bohets HH, Van Thielen MN, Van der Biest I, et al. Cytotoxicity of mercury compounds in LLC-PK1 MDCK and human proximal tubular cells. *Kidney Int*. 1995;47(2):395–403.
10. Nakazawa N, Makino F, Okada S. Acute effects of Mercury compounds on cultured mammalian cells. *Biochem Pharmacol*. 1975;24(4):489–493.
11. Zalups RK, Lash LH. Advances in understanding the renal transport and toxicity of mercury. *J Toxicol Environ Health*. 1994;42(1):1–44.
12. Bizarro P, Acevedo S, Nĩno-Cabrera G, et al. Ultrastructural modifications in the mitochondrion of mouse Sertoli cells after inhalation of lead, cadmium or lead–cadmium mixture. *Reprod Toxicol*. 2003;17(5):561–566.
13. Pfaller W, Gstraunthaler G, Willinger CC. Morphology of renal tubular damage from nephrotoxins. *Toxicol Lett*. 1990;53(1–2):39–43.
14. Magos L, Sparrow S, Snowden R. Effect of prolonged saline loading on $HgCl_2$-induced renal tubular damage. *Br J Exp Pathol*. 1984;65(5):567–575.
15. Cruz-Orive LM, Weibel ER. Recent stereological methods for cell biology: A brief survey. *Am J Physiol*. 1990;258:148–156.
16. Gundersen HJ, Bendtsen TF, Korbo L, et al. Some new, simple and efficient stereological methods and their use in pathological research and diagnosis. *Apmis*. 1988;96(5):379–394.
17. Tunç AT, Turgut M, Aslan H, Sahin B, Yurtseven ME, Kaplan S. Neonatal pinealectomy induces Purkinje cell loss in the cerebellum of the chick: a stereological study. *Brain Res*. 2006;1067(1):95–102.
18. Gundersen HJG, Jensen EB. The efficacy of systematic sampling in stereology and its prediction. *J Micros*. 1987;147(3):229–263.
19. Sterio DC. The unbiased estimation of number and sizes of arbitrary particles using the disector. *J Microsc*. 1984;134(2):127–136.
20. Kaplan S, Gökyar A, Unal B, Tunç AT, Bahadir A, Aslan H. A simple technique for localizing consecutive fields for dissector pairs in light microscopy: Application to neuron counting in rabbit spinal cord following spinal cord injury. *J Neurosci Met*. 2005;145(1–2):277–284.
21. Unal B, Özbek ME, Aydin MD, et al. Effect of haloperidol on the numerical density of neurons and nuclear height in the rat hippocampus: A stereological and histopathological study. *Neurosci Res Commun*. 2004;34(1):1–9.
22. Zahir F, Rizwi SJ, Haq SK, Khan RH. Low dose mercury toxicity and human health. *Environ Toxicol Pharmacol*. 2005;20(2):351–360.
23. Hussain S, Atkinson A, Thompson SJ, Khan AT. Accumulation of mercury and its effect on antioxidant enzymes in brain, liver, and kidneys of mice. *J Environ Sci Health B*. 1999;34(4):645–660.

24. Reus IS, Bando I, Andres D, Cascales M. Relationship between expression of HSP70 and metallothioneins and oxidative stress during mercuric chloride induced acute liver injury in rats. *J Biochem Mol Toxicol*. 2003;17(3):161–168.
25. Girardi G, Elias MM. Mercuric chloride effects on rat renal redox enzymes activities: SOD protection. *Free Radic Biol Med*. 1995;18(1):61–66.
26. Miura K, Naganuma A, Himeno S, Imura N. Mercury toxicity: Biochemical aspects. In: Goyer RA, Cherian G, eds. *Toxicology of Metals*. Berlin: Springer-Verlag; 1995:163–187.
27. Cantoni, O, Christie NT, Swann A, Drath DB, Costa M. Mechanism of $HgCl_2$ cytotoxicity in cultured mammalian cells. *Mol Pharmacol*. 1984;26(2):360–368.
28. Chung AS, Maines MD, Reynolds WA. Inhibition of the enzymes of glutathione metabolism by mercuric chloride in rat kidney: Reversal by selenium. *Biochem Pharmacol*. 1982;31(19):3093–3100.
29. Gastraunthaler G, Pfaller W, Kotanko P. Glutathione depletion and in vitro lipid peroxidation in mercury or maleate induced acute renal failure. *Biochem Pharmacol*. 1983;32(19):2969–2972.
30. Arvidson B, Arvidson J, Johansson K. Mercury deposits in neurons of the trigeminal ganglia after insertion of dental amalgam in rats. *Biometals*. 1994;7(3):261–263.
31. Eley BM. A study of mercury redistribution, excretion and renal pathology in guinea-pigs implanted with powdered dental amalgam for between 2 and 4 years. *J Exp Path*. 1990;71:375–393.
32. Hahn LJ, Klober R, Vimy MJ, Takahashi Y, Lorscheider FL. Dental ''silver'' tooth fillings: A source of mercury exposure revealed by whole-body image scan and tissue analysis. *FASEB J*. 1989;3(14):2641–2646.
33. Lentz DL, Buchanan JT, Zardiackas LD, Alexandre JJ. Mercury penetration into the pulp of teeth restored with amalgam. *Am J Dent*. 1989;2(4):171–173.
34. Altunkaynak ME, Ozbek E, Altunkaynak BZ, Can I, Unal D, Unal B. The effects of high-fat diet on the renal structure and morphometric parametric of kidneys in rats. *J Anat*. 2008;212(6):845–852.
35. Agarwal R, Goel SK, Chandra R, Behari JR. Role of vitamin E in preventing acute mercury toxicity in rat. *Environ Toxicol Phar*. 2010;29(1):70–78.
36. Eto K, Yasutake A, Miyamoto K, Tokunaga H, Otsuka Y. Chronic effects of methylmercury in rats. II. Pathological aspects. *Tohoku J Exp Med*. 1997;182(3):197–205.
37. Zalups RK, Gelein RM, Cernichiari E. DMPS as a rescue agent for the nephropathy induced by mercuric chloride. *J Pharmacol Exp Ther*. 1991;256(1):1–10.
38. Zalups RK, Barfuss DW. Nephrotoxicity of inorganic mercury co-administered with L-cysteine. *Toxicol*. 1996;109(1):15–29.
39. Li SJ, Zhang SH, Chen HP, et al. Mercury-induced membranous nephropathy: Clinical and pathological features. *Clin J Am Soc Nephrol*. 2010;5(3):439–444.
40. Opitz H, Schweinsberg F, Grossmann T, Wendt-Gallitelli MF, Meyermann R. Demonstration of mercury in the human brain and other organs 17 years after metallic mercury exposure. *Clin Neuropathol*. 1996;15(3):139–144.
41. Romero D, Gómez-Zapata M, Luna A, Garćıa-Fernández AJ. Comparison of cytopathological changes induced by mercury chloride exposure in renal cell lines (VERO and BGM). *Environ Toxicol Phar*. 2004;17(3):129–141.